

1 Measuring thermal performance in steady-state conditions at each stage of a full fabric retrofit to a solid wall  
2 dwelling

3 David Farmer <sup>a</sup>, Prof. Chris Gorse <sup>a</sup>, Prof. William Swan <sup>b</sup>, Dr. Richard Fitton <sup>b</sup>, Matthew Brooke-Peat <sup>a</sup>, Dominic  
4 Miles-Shenton <sup>a</sup>, Prof. David Johnston<sup>a</sup>

5 <sup>a</sup> Centre for the Built Environment, Leeds Sustainability Institute, Leeds Beckett University, BPA223  
6 Broadcasting Place, Woodhouse Lane, Leeds, LS2 9EN, UK

7 <sup>b</sup> Applied Buildings and Energy Research Group, School of Built Environment, University of Salford, Salford, M5  
8 4WT, UK

## 9 Abstract

10 The methodology used for measuring the thermal performance of fabric retrofit systems which were applied  
11 to a solid wall UK Victorian house situated within an environmental chamber is explored in detail. The work  
12 describes how steady-state boundary conditions were approximated, then repeated at the Salford Energy  
13 House test facility. How established methods of measuring the fabric thermal performance of buildings *in situ*  
14 were adapted to test the effectiveness of retrofit measures within a steady-state environment. The results  
15 presented show that steady-state boundary conditions enable the change in fabric heat loss resulting from the  
16 retrofit of a whole house or individual element to be measured to a level of accuracy and precision that is  
17 unlikely to be achieved in the field. The test environment enabled identification of heat loss phenomena  
18 difficult to detect in the field. However, undertaking tests in an environment devoid of wind underestimates  
19 the potential reduction in ventilation heat loss resulting from an improvement in airtightness, and hides the  
20 susceptibility of retrofit measures to various heat loss mechanisms, such as wind washing. The strengths and  
21 weaknesses of the methods employed, the Energy House test facility, and a steady-state environment, for  
22 characterising retrofit building fabric thermal performance are demonstrated.

## 23 Highlights

- 24 • First known measurement of HTC in steady-state conditions.
- 25 • Fabric retrofit thermal performance measured in steady-state conditions.
- 26 • Established thermal performance test methods adapted for steady-state measurement.
- 27 • Recommendations provided for assessing Energy House retrofit thermal performance.
- 28 • Strengths & weakness of the Energy House test facility for testing retrofit explored.

## 29 1. Introduction

30 *Table 1 – Nomenclature*

Term	Symbol	Unit
Whole building heat transfer coefficient	HTC	W/K
Thermal transmittance	U-value (U)	W/m <sup>2</sup> K
Target retrofit thermal transmittance	U <sub>t</sub>	W/m <sup>2</sup> K
Thermal conductivity	λ	W/mK
Thermal resistance	R-value (R)	m <sup>2</sup> K/W
Internal surface thermal resistance	R <sub>si</sub>	m <sup>2</sup> K/W
External surface thermal resistance	R <sub>se</sub>	m <sup>2</sup> K/W
Measured baseline thermal resistance	R <sub>b</sub>	m <sup>2</sup> K/W
Thermal resistance of retrofit materials	R <sub>m</sub>	m <sup>2</sup> K/W
Power input	Q	W
Heat flux density	q	W/m <sup>2</sup>
Internal air to external (chamber) air temperature difference	ΔT	K
Air permeability at 50 Pa	q <sub>50</sub>	m <sup>3</sup> .h <sup>-1</sup> .m <sup>2</sup> @ 50 Pa
Air change rate at 50 Pa	n <sub>50</sub>	h <sup>-1</sup> @ 50 Pa
Background ventilation rate	n	h <sup>-1</sup>
Ventilation heat transfer coefficient	HTC <sub>(v)</sub>	W/K
Internal surface area	A	m <sup>2</sup>

31 “Improving the energy efficiency of the existing [UK housing] stock is a long-term, sustainable way of ensuring  
32 multiple gains, including environmental, health and social gains.” (Marmot Review Team, 2011<sup>1</sup>). Pre-1919  
33 homes are ripe to yield the aforementioned gains as they comprise 21% of England’s housing stock and have  
34 the lowest average energy performance rating (DCLG, 2017<sup>2</sup>). However, these homes typically have solid wall  
35 construction (Everett, 2007<sup>3</sup>) and it is not currently considered economically viable to the apply solid wall  
36 insulation required to make them energy efficient (Galvin and Sunikka-Blank, 2017<sup>4</sup>).

37 The incentive to perform retrofit is further diminished as the anticipated reductions in energy use are often  
38 not realised (Gupta *et al.*, 2015<sup>5</sup>). This has been attributed to incorrect assumptions regarding occupant energy  
39 use behaviour pre-retrofit (Sunikka-Blank and Galvin, 2012<sup>6</sup>) and post-retrofit (Galvin, 2014<sup>7</sup>). Evidence is also  
40 growing to suggest that assumptions regarding heat loss from a home pre- and post-retrofit are incorrect. UK  
41 Government schemes to incentivise retrofit such as the Energy Company Obligation (ECO) (OFGEM, 2015<sup>8</sup>) and  
42 the now defunct Green Deal (Dowson *et al.*, 2012<sup>9</sup>) calculate baseline thermal performance using the Reduced  
43 Data Standard Assessment Procedure (RdSAP) (BRE, 2012<sup>10</sup>). The average measured heat loss from solid walls  
44 has been found to be substantially less than the standard values used by the RdSAP calculation (BRE, 2014<sup>11</sup>  
45 and Li *et al.*, 2015<sup>12</sup>), meaning the baseline heat loss prediction could be overestimated. A performance gap  
46 between the measured and predicated reduction in heat loss from fabric retrofit measures has also been  
47 observed (Doran, 2008<sup>13</sup> and Miles-Shenton *et al.*, 2011<sup>14</sup>). Thus, it can be argued that more measurements  
48 should be undertaken pre- and post-retrofit to understand the nature of the prediction and performance gaps  
49 in retrofit.

50 The effectiveness of a thermal retrofit can be assessed at a whole building level by measuring the change in  
51 heat transfer coefficient (HTC). ISO 13789 defines the HTC as the “heat flow rate divided by temperature  
52 difference between two environments” (BSI, 2007<sup>15</sup>). It represents the steady-state aggregate total fabric and  
53 ventilation heat transfer coefficient ( $HTC_{(v)}$ ) from the entire thermal envelope in Watts, per kelvin of  
54 temperature difference ( $\Delta T$ ) between the internal and external environments, and is expressed in W/K. The  
55 coheating test has been shown to be reliable a reliable method of determining the HTC of a building (Jack *et*  
56 *al.*, 2017<sup>16</sup>). The improvement in HTC resulting from retrofit has been measured using coheating tests by Miles-  
57 Shenton *et al.* (2011<sup>14</sup>) and Rhee-Duverne and Baker (2013<sup>17</sup>). In both instances the baseline HTC measured  
58 was lower than that predicted using RdSAP, which highlights the importance of calculating potential  
59 improvements in thermal performance from a measured baseline. Miles-Shenton *et al.* found performance  
60 gaps between the measured and predicted HTC reduction at each stage of the retrofit process. However, HTC  
61 measurements are not targeted enough to explain the cause of a performance gap.

62 The thermal transmittance of a building element (U-value) is defined in ISO 7345 as the “Heat flow rate in the  
63 steady state divided by area and by the temperature difference between the surroundings on both sides of a  
64 flat uniform system” (BSI 2017<sup>18</sup>). Measurement of *in situ* U-values is typically undertaken in accordance with  
65 ISO 9869 (BSI, 2014<sup>19</sup>). Doran (2008<sup>13</sup>) and Miles-Shenton *et al.* (2011<sup>14</sup>) both measured U-value performance  
66 gaps for retrofitted cavity wall insulation (CWI). Miles-Shenton *et al.* found that U-value performance gaps  
67 measured for the CWI retrofit and for the subsequent external wall insulation (EWI) retrofit were sufficient to  
68 account for the discrepancy between the measured and predicted HTC reduction following each retrofit.

69 Work undertaken by Everett (1985<sup>20</sup>) and Stamp *et al.* (2013<sup>21</sup>, 2017<sup>22</sup>) investigating the coheating test method  
70 uncovered a number of variables that not only increase the complexity of the data analysis, but can also result  
71 in greater uncertainty. Variables identified include: inaccurate estimation of solar gains, delayed release of  
72 stored solar gains from the thermal mass, variation in air infiltration (background ventilation rate ( $n$ )) caused  
73 by a change in wind velocity and/or direction, thermal lag caused by external temperature variation, long-  
74 wave radiative heat exchange with the sky, solid ground floor heat loss not directly driven by the internal air-  
75 to-external air  $\Delta T$ , and inter-dwelling heat transfer across a party wall. Many of these variables are also known  
76 to increase the uncertainty of *in situ* U-value measurements. The variables listed are all caused by variations in  
77 the external boundary conditions and, with the exception of inter-dwelling heat transfer, cannot be practically  
78 controlled. The effects of solar radiation on the building fabric mean that it is recommended that coheating  
79 tests are only undertaken during the winter months.

80 As a consequence, it is accepted that when measuring the thermal performance of an unoccupied house, the  
81 main sources of uncertainty result from variations in the external boundary conditions. This problem is  
82 compounded when attempting to measure the improvement in thermal performance resulting from thermal  
83 retrofit, due to the uncertainty associated with both the pre- and the post-retrofit measurements. Coheating  
84 test accuracy is estimated to be  $\pm 8\text{--}10\%$  (Jack *et al.*, 2017<sup>16</sup>). The uncertainty of *in situ* U-value measurements  
85 undertaken in accordance with ISO 9869 is quoted as  $\pm 14\%$  (BSI, 2014<sup>19</sup>). The uncertainty of air permeability  
86 ( $q_{50}$ ) measurements using a blower door is highly dependent upon the wind velocity, with the uncertainty  
87 ranging from  $<\pm 2\%$  in calm conditions and  $\pm 15\%$  at a velocity of 6 m/s (Persilly, 1982<sup>23</sup>), the maximum velocity  
88 in which measurements can be undertaken in accordance with ATTMA Technical Standard L1 (ATTMA, 2016<sup>24</sup>).  
89 Such levels of measurement uncertainty can make it difficult to confidently measure minor improvements in  
90 building fabric thermal performance. Additionally, if the analysis of the test data does not account for any  
91 major difference in external boundary conditions, experienced during the pre- and post-retrofit test periods,  
92 then the measured difference in thermal performance could be misleading. Both Miles-Shenton *et al.* (2011<sup>14</sup>)  
93 and Rhee-Duverne and Baker (2013<sup>17</sup>) reported notable differences in the external boundary conditions  
94 present during a series of pre- and post-retrofit tests, particularly regarding solar radiation and wind  
95 respectively. In an coheating test, solar radiation and wind velocity are included as independent variables in  
96 the multiple regression analysis to try to normalise for any difference in these variables that is experienced  
97 between the tests. However, it is recognised that the analysis techniques employed on coheating data are  
98 often unable to isolate the effect of many of the physical phenomena present during a test (Bauwens *et al.*  
99 2014<sup>25</sup>).

100 One way to eliminate the uncertainties caused by variations in external boundary conditions is to perform  
101 measurements at a steady-state within a laboratory setting. Hot boxes have been used since the 1970s to  
102 create steady-state conditions to reliably measure the thermal performance of many building components  
103 (Asdrubali and Baldinelli, 2011<sup>26</sup>). However, it is only since the opening of the Salford Energy House test facility  
104 in 2011 that it has been possible to undertake steady-state thermal performance measurements on an entire  
105 building. The work presented in this paper details the first HTC measurements of a building in steady-state  
106 conditions and the improvement in thermal performance resulting from the application of a range of fabric  
107 retrofit systems. The methodology describes in detail how steady-state boundary conditions were  
108 approximated and repeated and how recognised methods for measuring the fabric thermal performance of  
109 buildings *in situ* were adapted to test the effectiveness of retrofit measures within a steady-state environment.  
110 The analysis of the test results is primarily focused on assessing the utility of the Energy House test facility for  
111 measuring retrofit thermal performance and identifying any potential causes of underperformance using  
112 established measurement techniques. It is hoped that the work presented in this paper will provide those  
113 undertaking similar work at the Energy House, or other similar full-scale indoor test facilities, and to a lesser  
114 extent in the field, with guidance for conducting experiential work and interpreting their findings.

## 115 **2. Methodology**

### 116 **2.1 The Salford Energy House Test Facility**

117 The Salford Energy House (Figure 1) is a full scale replica pre-1919 solid-wall Victorian end-terrace house  
118 constructed inside an environmentally controlled chamber at the University of Salford. The construction of the  
119 Energy House was achieved using reclaimed materials and methods of the time, it shares a party wall with an  
120 adjacent house (Guard House). Details of the baseline Energy House construction are provided in Table 2.



121  
122 *Figure 1 – The Salford Energy House*

123 *Table 2 - Baseline Energy House construction details*

Thermal element	Construction
External walls	Solid wall – 222.5 mm brick arranged in English bond (5 courses) with 9 mm lime mortar and 10.5 mm British Gypsum Thistle hardwall plaster with a 2 mm Thistle Multi-Finish final coat. The ground and intermediate floor joists are built-in to the gable wall.
Roof	Purlin and rafter cold roof structure with insulation at ceiling level. 100 mm existing mineral wool insulation ( $\lambda$ 0.044 W/mK) between 100x50 mm ceiling joists running parallel to the gable wall at 400 mm centres above lath (6 mm) and plaster (17 mm) ceiling.
Ground floor	Suspended timber ground floor above a ventilated underfloor void (20 mm depth). 150x22 mm floor boards fixed to 200x50 mm floor joists at 400 mm centres. Floor joists run between the gable and party wall with joists ends built into masonry walls.
Windows	Double glazed units in PVCu frames fitted with trickle vents. Typical of 1980's replacement double glazing ( <b>single glazed timber sash windows were present during the preliminary experiment</b> ).
Doors	UPVC of amid range type, again typical of a 1980's replacement ( <b>uninsulated timber doors units with single glazing were present during the preliminary experiment</b> ).
Party wall	Solid wall – same as external walls, except unplastered on the Guard House side.

124 The environmental chamber is a large reinforced concrete structure. The chamber walls are insulated with 100  
125 mm PIR foam insulation to the walls and ceiling and 35 mm expanded polystyrene insulation to the floor  
126 element (reinforced concrete slab on short bored piles). The chamber has the ability to maintain a constant  
127 temperature between the range -12 °C and +30 °C with an accuracy of  $\pm 0.5$  °C at a 5 °C set-point. The chamber  
128 is cooled by an air handling unit that is supplied with cooling by four condenser units, with a total of 60 kW of  
129 cooling (15 kW per unit). This is supplied to the chamber via a ducted heating, ventilation, and air conditioning  
130 (HVAC) system. This system reacts to the heat load of the house in the chamber and maintains a set-point of  $\pm$   
131 0.5 °C.

## 132 **2.2 Test programme and experimental design**

### 133 **2.2.1 Preliminary experiment**

134 A preliminary experiment was undertaken to measure the heat transfer coefficient (HTC) of the Salford Energy  
135 House at a range of  $\Delta T$ 's considered typical of those that are likely to be encountered in the North West of  
136 England during the coheating test heating season (October – March). The experiment was designed to test the  
137 assumption whether a linear relationship exists between Q and  $\Delta T$  and to establish whether HTC  
138 measurements of the Energy House within the selected range of  $\Delta T$ 's are significantly affected by differences  
139 in radiative heat exchange with the chamber fabric and apparatus, and stack effect driven n. Most pertinent to  
140 the work contained within this paper, the preliminary experiment would determine the validity of measuring  
141 the Energy House HTC at a single  $\Delta T$  prior to undertaking the retrofit experiment.

142 The limited test duration allocated to the preliminary experiment (eight days, plus a three-day heat-up and  
143 instrumentation period) resulted in only three different steady-state  $\Delta T$  periods being considered (10 K, 15 K

144 and 20 K). Time constraints also meant that it was only possible to undertake the HTC measurements during  
 145 the final eight hours of each steady-state  $\Delta T$  period. The thermostatic heating controllers in the Energy House  
 146 and the adjacent Guard House were set to maintain an internal air temperature of 25 °C, as recommended by  
 147 the 2010 Leeds Beckett University Whole House Heat Loss Test Method (Wingfield *et al.*, 2010<sup>27</sup>). The chamber  
 148 HVAC was initially set to maintain an air temperature of 15 °C during the initial steady-state measurement  $\Delta T$   
 149 period. Subsequently, the chamber air temperature set-point was reduced on two further occasions to 10 °C  
 150 and 5 °C, thus increasing the  $\Delta T$ .

151 **2.2.2 Retrofit experiment**

152 The purpose of the retrofit experiment was to quantify the impact that a full fabric retrofit would have on the  
 153 building fabric thermal performance of the Energy House using commercially available thermal upgrade  
 154 measures. Therefore, the experiment was designed to enable the change in building fabric thermal  
 155 performance resulting from the application of the various retrofit measures when applied individually, or in  
 156 combination, to be measured; as well as identify and investigate the cause for any discrepancy between the  
 157 calculated and measured thermal performance of the various retrofit measures.

158 The Energy House underwent a staged retrofit process with the thermal elements of the Energy House being  
 159 retrofitted individually, or in combination. For practical reasons, it was deemed appropriate to undertake the  
 160 full retrofit first, then remove or replace individual thermal retrofit measures throughout each stage of the  
 161 experiment. However, given the time constraints associated with the experiment, it was not possible to  
 162 measure the ground floor retrofit in isolation. The configuration of the Energy House at each stage of the  
 163 experiment is provided in Table 3.

164 *Table 3 - Energy House configuration at each test stage of the retrofit experiment (shading represents retrofit*  
 165 *installed)*

Test stage	Condition of thermal element at each test stage			
	External wall	Roof	Glazing	Floor
1 (Full retrofit)	Hybrid solid wall insulation system	270 mm mineral wool	A+++ glazing, argon fill, low e	200 mm mineral wool + membrane
2 (Full retrofit with original floor)	90 mm EPS EWI to gable and rear walls			
3 (Solid wall)	80 mm PIR IWI to front wall	100 mm mineral wool	1980s style double glazing units	
4 (Glazing)			A+++ glazing, argon fill, low e	Uninsulated (suspended timber)
5 (Roof)	Uninsulated (solid wall)	270 mm mineral wool	1980s style double glazing units	
6 (Baseline)		100 mm mineral wool		

166 Measurements of building fabric thermal performance were undertaken at each stage of the experiment, with  
 167 the most relevant to the work presented here being the steady-state HTC, the *in situ* U-value measurements  
 168 and  $q_{50}$  measurements. These measurements provided either the baseline or retrofit value for each thermal  
 169 element. The change in thermal performance attributable to the retrofit of each thermal element was  
 170 calculated as the difference between the measured retrofit and the baseline values. As the retrofit process was  
 171 performed in reverse order, the retrofit value was measured prior to the baseline value. Unfortunately, this

172 had the effect of limiting the analysis that could be undertaken during the experiment to identify the cause for  
173 any underperformance measured.

174 The average internal and external air temperatures experienced by houses situated in North West England  
175 during the heating season were chosen for the retrofit experiment. The chamber HVAC system was set to  
176 maintain an air temperature of 5 °C. This was based on findings from the preliminary experiment relating to  
177 the behaviour of the chamber's HVAC temperature control system (refer to section 3.1), and its proximity to  
178 the mean external air temperature for North West England during the October to May heating season  
179 contained within the Standard Assessment Procedure of 6.6 °C (BRE, 2012<sup>10</sup>). The thermostatic heating  
180 controllers in the Energy House and the adjacent Guard House were set to maintain an internal air  
181 temperature of 20 °C. This temperature was selected as it is the average central heating thermostat set-point  
182 for homes in England (Shipworth *et al.*, 2010<sup>28</sup>). It was considered acceptable to reduce the internal  
183 temperature from the coheating test method recommendation of 25°C selected for the preliminary  
184 experiment, as the test environment guarantees a positive ΔT throughout the duration of a coheating test.  
185 Thus, a 15 K ΔT was maintained during the retrofit experiment.

## 186 2.3 Thermal performance measurements

### 187 2.3.1 Heat transfer coefficient (HTC)

188 The Energy House HTC was measured using an coheating test. In the field, the coheating test is termed a  
189 'quasi-steady-state' test method and while the elevated, stable, and homogenous air temperature present  
190 within the internal environment during a coheating test facilitates a steady-state condition, the variation in  
191 weather experienced in the field means that in practice it is unlikely that a test house will ever be at steady-  
192 state. Hence, a typical measurement period of between one and three weeks is required to reduce the effects  
193 of thermal mass, and to estimate the power input from solar radiation using linear regression techniques.  
194 However, the control of the external boundary conditions at the Energy House test facility makes steady-state  
195 measurements possible and within a shorter period of time than would normally be required within the field.

196 The coheating test typically assumes the steady-state whole house energy balance in Equation (adapted from  
197 Everett, 1985<sup>20</sup>).

$$198 \quad Q + R.S = (\Sigma U.A + C_v). \Delta T \quad [1]$$

199 Where: R = Solar aperture of the house (m<sup>2</sup>)  
200 S = Solar irradiance (W/m<sup>2</sup>)

201 At the Energy House test facility, the terms R and S can be removed from the whole house energy balance, and  
202 the equation rearranged to show how at steady-state, the HTC can be calculated from measurements of just Q  
203 and ΔT. Equation 2 shows the HTC calculation for each steady-state measurement.

$$204 \quad HTC = \frac{Q}{\Delta T} \quad [2]$$

205 No formally recognised standard currently exists for undertaking an coheating test. The 2010 Leeds  
206 Metropolitan (now Beckett) University Whole House Heat Loss Test Method became recognised as an  
207 established test method in the UK when it was incorporated within the Post Construction and Initial  
208 Occupation studies undertaken under the Technology Strategy Board's (now Innovate UK's) Building  
209 Performance Evaluation Programme (TSB, 2010<sup>29</sup>). This method was adapted to undertake the HTC  
210 measurements in the preliminary experiment. The 2013 version of the test method (Johnston *et al.*, 2013<sup>30</sup>)  
211 was adapted to undertake HTC measurements in the retrofit experiment. The test methods were adapted to  
212 account for a steady-state environment, the most notable changes being a shorter test duration (refer to  
213 section 2.3.4), an alternative analysis method and no requirement for a weather station.

214 The internal environment of the Energy House and adjacent Guard House were heated using portable electric  
215 resistance heaters placed in each zone (room), with each heater being capable of providing 750 W, 1250 W, or  
216 2000 W of heat input. Each heater was controlled by a PID thermostatic temperature controller with a PT100  
217 RTD temperature sensor (accuracy ± 0.1 K), which was set to maintain an air temperature in each zone of 25 °C  
218 during the preliminary experiment and 20 °C during the retrofit experiment. An electrically driven air

219 circulation fan was placed in each zone and the internal doors were left open to increase air temperature  
220 homogeneity. Power input (Q) from the heaters, fans, and logging equipment was measured by a Wh energy  
221 meter (uncertainty  $\pm 1\%$ ). The internal temperature in each zone was measured with a PT100 RTD  
222 temperature sensor (accuracy  $\pm 0.1$  K) positioned in the centre of each zone at mid-storey height. The chamber  
223 air temperature was measured using PT100 RTD temperature sensors (accuracy  $\pm 0.1$  K) positioned at the mid-  
224 storey height of the ground floor and first floor on each elevation. The internal air temperature of the Guard  
225 House was also maintained at the same temperature as the Energy House in each experiment, in order to  
226 minimise inter-dwelling heat transfer across the party wall. Energy consumption, along with internal and  
227 chamber environmental data, were logged throughout the experiments using an Eltek Squirrel RX250AL data  
228 logger. Missing data ( $\sim 10\%$ ) were corrected using linear interpolation. Measurements were recorded at  
229 intervals of ten minutes throughout the preliminary experiment and one minute throughout the retrofit  
230 experiment.

231 As very little variation in the mean internal air temperature was measured between the rooms during the  
232 preliminary and the retrofit experiment, the  $\Delta T$  was obtained by subtracting the arithmetic mean internal  
233 temperature of the Energy House from the arithmetic mean chamber temperature. Uncertainty for each HTC  
234 measurement was calculated by error propagation of the uncertainty associated with measured Q and the SD  
235 of the internal and chamber air temperature measurements used to calculate  $\Delta T$ .

### 236 2.3.2 *In situ* U-value and R-value measurements

237 *In situ* U-value measurements were generally undertaken in accordance with ISO 9869 (BSI, 1994<sup>31</sup>), however  
238 the analysis period was shortened due to the measurements being undertaken within a steady-state  
239 environment (refer to section 2.3.4). *In situ* U-values were calculated for each steady-state measurement using  
240 Equation 3 adapted from ISO 9869. Thermal resistance (R-value) was obtained by taking the reciprocal of the  
241 U-value.

$$242 \quad U = \frac{q}{\Delta T} \quad [3]$$

243 Heat flux density (q) was measured using Hukseflux HFP01 (uncertainty  $\pm 3\%$ ) heat flux plates (HFPs) installed  
244 at 75 locations on the thermal elements of the Energy House during the retrofit experiment. HFPs were  
245 positioned, with the aid of thermography, in locations considered to be representative of each element. The  
246 HFPs were affixed to surfaces using adhesive tape and thermal contact paste. The voltage induced by the HFPs  
247 was recorded at one minute intervals by a Thermo Fisher Scientific dataTaker DT80 data logger. *In situ* U-  
248 values were corrected to account for the R-value of the HFP ( $6.25 \times 10^{-3} \text{ m}^2\text{K/W}$ ). The air circulation fans were  
249 positioned to avoid them blowing directly onto HFPs. The air-to-air  $\Delta T$  was measured in the vicinity of each  
250 HFP location using PT100 RTD temperature sensors.

251 The baseline and retrofit *in situ* U-value reported for entire thermal elements were calculated as the mean of  
252 the individual *in situ* U-values measured on a thermal element at locations deemed uncompromised by  
253 thermal bridging at junctions with neighbouring thermal elements (typically distances  $> 1$  m from junctions as  
254 heat flow  $\leq 1$  m is included in thermal bridging calculations). Uncertainty for each *in situ* U-value measurement  
255 was calculated by error propagation of the uncertainty associated with the measured variables q and  $\Delta T$  in  
256 Equation 3.

257 The target retrofit U-value for elements which were thermally upgraded (rather than replaced) were  
258 calculated using Equation 4. The additional R-value provided by the retrofit materials was calculated in  
259 accordance with ISO 6946 (BSI, 2007<sup>32</sup>) using values for  $\lambda$  and material thicknesses provided by the  
260 manufacturers' product datasheets.

$$261 \quad U_t = \frac{1}{R_b + R_m} \quad [4]$$

### 262 2.3.3 Blower door tests

263 Blower door tests in accordance with ATTMA Technical Standard L1 were performed at each stage of the  
264 retrofit experiment. The tests were undertaken to measure the change in  $q_{50}$  resulting from each retrofit  
265 measure, to induce a pressure differential between the Energy House and chamber to enable air infiltration

266 points to be identified with thermography, detect any potential air movement within the building fabric using  
267 HFPs and temperature sensors, and to estimate  $n$ . The chamber doors were left open throughout each test to  
268 equalise the pressure between the chamber and external environment. Based on the assumption of zero wind  
269 velocity within the chamber the uncertainty associated with each measurement is  $\pm 2\%$ , this value is based on  
270 the findings of Persily (1982<sup>23</sup>).

271 The air change rate at 50 Pa ( $n_{50}$ ) measured at each stage of the retrofit experiment was used to approximate  
272  $n$  of the Energy House using the  $n_{50}/20$  'rule of thumb' (Kronvall, 1978<sup>33</sup>), adjusted to  $n_{50}/19.2$  to account for  
273 storey height and sheltering factor (Sherman, 1987<sup>34</sup>). Typically, a single zone trace gas technique such as that  
274 detailed by Roulet and Foradini (2002<sup>35</sup>) is also used to determine  $n$  during tests in the field. However, it was  
275 found during the preliminary experiment that the  $\text{CO}_2$  released into the test house moved in a cycle between  
276 the Energy House and the chamber, thus precluding the use of a single zone tracer gas decay method for the  
277 retrofit experiment. Unfortunately, a multi-zone tracer gas measurement was not available to the research  
278 team.

279 The approximated  $n$  was multiplied by the internal volume of the Energy House and by the specific heat  
280 capacity of air ( $0.33 \text{ Wh/m}^3\text{K}$ ) to determine  $\text{HTC}_{(V)}$  ( $\text{W/K}$ ) by. Subtracting  $\text{HTC}_{(V)}$  from the measured HTC enables  
281 the HTC to be disaggregated into its fabric and ventilation components.

### 282 2.3.4 Repeatable steady-state measurements at the Energy House test facility

283 ISO 9251 defines a steady-state as a "*Condition for which all relevant parameters do not vary with time*" (BSI  
284 1987, p.1<sup>36</sup>). In practice, steady-state boundary conditions can only be approximated, as it is not possible to  
285 create a true steady-state due to the limitations of existing apparatus to accurately control and measure such  
286 an environment. Hence, the existence of standards which define the requirements for practicable  
287 determination of steady-state heat transfer. No recognised standard currently exists which defines the  
288 requirements for steady-state boundary conditions for the measurement of heat transfer (whole house or  
289 elemental) using an indoor full-scale test facility. The standards for steady-state U-value measurement using a  
290 guarded hot box and for *in situ* measurements undertaken in the field are ISO 8990 (BSI, 1996<sup>37</sup>) and ISO 9869-  
291 1 (BSI, 2014<sup>19</sup>) respectively. However, neither standard is considered appropriate for the Energy House test  
292 facility, as unlike measurements taken in the field, the internal and external boundary conditions can be  
293 controlled and repeated, but not to the precision or accuracy that can be achieved in a guarded hot box due to  
294 the scale of the Energy House test facility. The relevant boundary condition requirements for measurements to  
295 comply with ISO 8990 and ISO 9869 relate to: air temperature fluctuation and variation, heat content,  
296 moisture distribution and air velocity. These requirements, as well as test duration, will now be considered in  
297 regard to the Energy House test facility.

298 ISO 8990 requires temperature fluctuations to be kept within 1% of the air-to-air  $\Delta T$  when determining the  
299 steady-state thermal transmittance of building components in a guarded hot box. ISO 9869 contains no such  
300 requirement, as *in situ* U-value measurements in the field experience a diurnal temperature fluctuation  
301 externally and potential internal fluctuations resulting from space heating patterns in occupied dwellings.  
302 Therefore, it can be argued that given the close control of the internal temperature fluctuations during a  
303 coheating test of  $\pm 0.1 \text{ K}$ , and the regular chamber air temperature fluctuation of  $\pm 0.5 \text{ K}$ , a fluctuation in the  
304 air-to-air  $15 \text{ K } \Delta T$  of 3% can be considered close to what is considered practicable at a whole house scale.

305 ISO 8990 states that air temperature variation across a specimen surface should to not exceed 2% of the air-to-  
306 air  $\Delta T$ . Coheating test equipment creates a reasonably homogenous air temperature within each zone,  
307 resulting in a typical floor to ceiling air temperature gradient of  $\sim 0.3 \text{ K}$ . However, the internal arrangement of  
308 the first floor in the Energy House means that achieving a homogenous internal air temperature throughout  
309 the Energy House is challenging. Consequently, a variation in air temperature of up to  $1 \text{ K}$  between zones  
310 within the Energy House could be expected. An air temperature variation of up to  $1 \text{ K}$  within the chamber is  
311 considered typical. If the thermal envelope of the Energy House is considered to constitute the specimen  
312 surface for HTC measurements, then the variation in air-to-air  $\Delta T$  is  $\leq 9\%$ , which far exceeds that required by  
313 ISO 8990. However, in the event that internal air temperature variation throughout the Energy House was  
314 reduced to zero, the variation in chamber air temperature alone would result in an air temperature variation  
315 exceeding 2% across the entire thermal envelope at. This suggests that the 2% limit detailed in ISO 8990 is not



316 practicable for an Energy House HTC measurement at a 15 K  $\Delta T$  (a 65 K  $\Delta T$  would be required to meet the 2%  
317 limit). To reconcile this potential source of measurement error, the variation in air temperature measured  
318 internally and within the chamber was included in the uncertainty calculation for each HTC measurement. To  
319 compensate for the variation in internal and chamber air temperatures, the  $\Delta T$  for *in situ* U-value  
320 measurements was measured locally, which fulfils the requirements of ISO 8990 and ISO 9869.

321 The fluctuation in  $\Delta T$  causes a fluctuation in the heat flow rate throughout a measurement, thus precluding an  
322 instantaneous steady-state measurement. However, averaging the heat flow rate and  $\Delta T$  over a sufficient  
323 period of time can smooth out the effects of these fluctuations. An averaging period of 24 hours was chosen,  
324 as it enables analysis of *in situ* U-value measurements be undertaken in accordance with ISO 9869 and is  
325 greater than the minimum period of three hours required by ISO 8990. Comparison can then be made  
326 between successive averaging periods to determine whether the heat flow rate can be considered constant,  
327 thus approximating to a steady-state.

328 The high thermal mass of the external walls and foundation slab of the Energy House means that charging or  
329 discharging of the thermal mass could be occurring even when a constant  $\Delta T$  is being measured. To ascertain  
330 whether the heat flow rate was constant prior to steady-state measurements, a stabilisation period existed in  
331 which a constant  $\Delta T$  was maintained and Q into the Energy House monitored. The stabilisation period ended  
332 once the average Q measured over a 24 hour period differed by less than  $\pm 5\%$  from that measured during the  
333 previous 24 hour period; at this point the heat flow rate was considered to be close to steady-state.

334 A steady-state test period of 72 hours in duration followed each stabilisation period, during which the  
335 chamber and Energy House were left undisturbed. A 72 hour test duration was chosen as it is the minimum  
336 test duration at a stable  $\Delta T$  required for *in situ* U-value measurements to comply with ISO 9869 (BSI, 2014<sup>29</sup>) if  
337 required. Each steady-state test period comprised two components, an initial period of 48 hours to allow any  
338 perturbations in the heat flow rate caused by disturbances to the test environment during the stabilisation  
339 period (e.g. visits by researchers) to settle. This was followed by a 24 hour period in duration when the  
340 reported steady-state measurements were undertaken. The steady-state measurements undertaken during  
341 the final 24 hours of a test were only considered valid if they differed by less than  $\pm 5\%$  from those measured  
342 during the previous 24 hour period. The  $\pm 5\%$  from the previous 24 period criterion is based upon one of the  
343 conditions for fulfilling the requirements of ISO 9869 for *in situ* U-value measurements, but greater than the  $\pm$   
344 1% between successive measurements required by ISO 8990. Without the time constraints imposed on the  
345 experiment, a stricter criterion would have been specified. Although the 24 hour measurement period is less  
346 than that stipulated by ISO 9869 (BSI, 2014<sup>29</sup>), it can be justified, as the 72 hour period stated by ISO 9869 is  
347 based upon three diurnal temperature cycles. As the chamber air temperature cycles at a frequency of  $\sim 20$   
348 minutes, it can be argued that each 24 hour period is equivalent to  $\sim 72$  diurnal cycles. Additionally, the  
349 undisturbed test environment during the prior 48 hour period increased the likelihood of achieving a steady-  
350 state.

351 The requirement to return the Energy House to its 'as found' condition following each experiment meant that  
352 it was not possible to measure moisture content or distribution within the building fabric of the Energy House  
353 to detect whether any changes were taking place. The sheltered test environment meant that the only  
354 noteworthy source of additional moisture that the building fabric of the Energy House was exposed to during  
355 the experiment was the wet plaster finish applied to the IWI on the front wall during Phase 1. In lieu of a direct  
356 measurement, RH measurements of the internal and chamber air were taken as a proxy. Air temperature set-  
357 points close to 0 °C were ruled out during experimental planning to ensure that any phase changes would not  
358 affect the measurements.

359 The continuous operation of air circulation fans within the Energy House and the chamber HVAC equipment  
360 ensured a constant air velocity across the internal and external surfaces of the Energy House during each  
361 steady-state measurement. Thus, any change in n following alteration to the building fabric can be attributed  
362 to a change in the airtightness of the Energy House. The location and speed setting of each air circulation fan  
363 remained unchanged throughout each experiment to ensure the internal surface thermal resistance ( $R_{si}$ ) and  
364 external surface thermal resistance ( $R_{se}$ ) were consistent between test stages.  $R_{si}$  and  $R_{se}$  were measured on  
365 each element throughout the retrofit experiment to identify whether any change occurred.

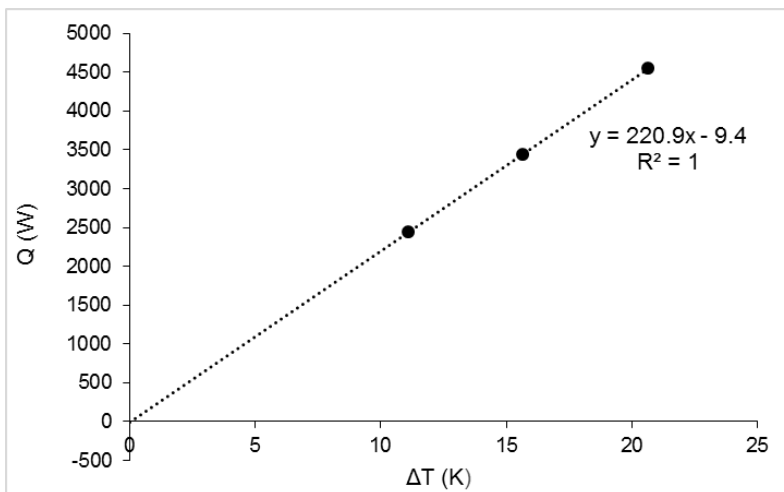
366 **3. Results and discussion**  
 367 **3.1 Preliminary experiment**

368 Table 4 provides the  $\Delta T$ , Q, and HTC measured during each steady-state measurement period in the  
 369 preliminary experiment.

370 Table 4 - Measured  $\Delta T$ , Q, and HTC for each steady-state measurement period of the preliminary experiment  
 371 (differences in HTC calculated using table values are due to rounding)

$\Delta T$ (K)	Q (W)	HTC (W/K)
11.1	2440	220.2 ( $\pm 10$ )
15.6	3441	220.0 ( $\pm 7.8$ )
20.7	4555	220.5 ( $\pm 7.1$ )

372 Table 4 shows that there was no significant difference between HTC measurements of the Energy House at  
 373 each steady-state  $\Delta T$ . Figure 2 shows the relationship between measured  $\Delta T$  and Q during each steady-state  
 374  $\Delta T$  measurement period.



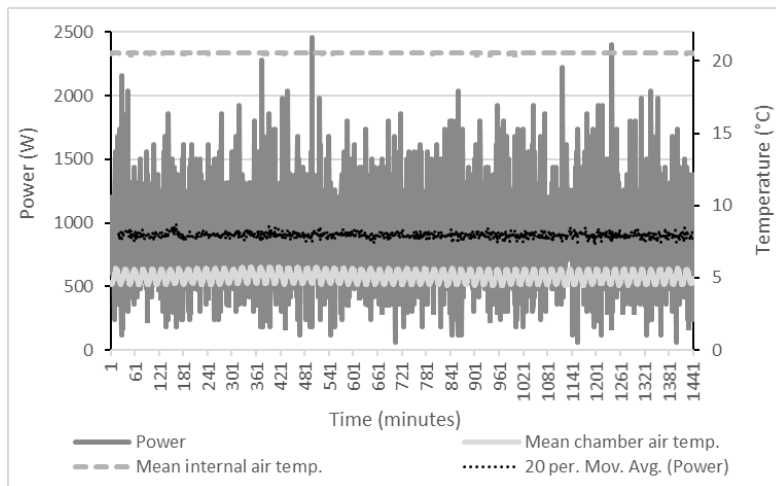
375  
 376 *Figure 2 - Relationship between measured  $\Delta T$  and Q during each steady-state  $\Delta T$  measurement period in the*  
 377 *preliminary experiment*

378 Figure 2 shows a perfect  $R^2$  linear correlation between  $\Delta T$  and Q measured during each steady-state  
 379 measurement period. The linear regression derived HTC of 220.9 ( $\pm 0.8$ ) W/K is in good agreement with that  
 380 measured at each steady-state  $\Delta T$ . This suggests that any differences in radiative heat exchange and stack  
 381 effect over the  $\Delta T$  range measured did not significantly affect the HTC measurement of the Energy House.  
 382 Therefore, the use of a single  $\Delta T$  within the measurement range used in the preliminary experiment can be  
 383 considered appropriate to measure the HTC of the Energy House.

384 The preliminary experiment also found that the chamber HVAC system achieved the greatest level of  
 385 temperature control with a 5 °C set-point. The chamber air temperature oscillated around the 5 °C set-point  
 386 with an amplitude of 0.5 °C with regular frequency of ~20 minutes. This suggests that steady-state  
 387 measurements of the Energy House HTC should be undertaken with a chamber set-point of 5 °C.

388 **3.1.1 Retrofit experiment**  
 389 **3.1.1.1 HTC measurements**

390 Figure 3 shows Q into the Energy House and mean internal and chamber air temperatures measured  
 391 throughout the full retrofit HTC steady-state measurement.



392  
393 *Figure 3 - Q and mean internal and chamber temperatures measured during the full retrofit HTC steady-state*  
394 *measurement*

395 A stable internal air temperature close to the 20 °C set-point and the regular chamber air temperature  
396 oscillation around the 5 °C set-point are evident in Figure 3. This indicates that, as far as can be considered  
397 practicable at the Energy House test facility, a steady-state  $\Delta T$  was present. A large variation in Q is also  
398 evident, however, the 60 minute moving average of Q indicates that the rate of heat flow was generally stable.  
399 Similar behaviour was observed throughout the measurement periods at each stage, providing confidence of a  
400 consistent test environment close to steady-state throughout the entire retrofit experiment.

401 Table 5 provides the HTC measurements for each stage of the retrofit experiment and the contribution of each  
402 thermal element retrofit to the reduction in HTC from baseline resulting from the full retrofit.

403 *Table 5 - HTC measured at each stage of the retrofit experiment and contribution of each thermal element*  
404 *retrofit to the reduction in HTC from baseline resulting from the full retrofit*

Test stage	HTC (W/K)	Reduction on baseline (W/K)	Contribution of each thermal element retrofit towards full retrofit HTC reduction (%)
1 (Full retrofit)	69.7 ( $\pm$ 2.4)	117.8	n/a
2 (Full retrofit with original floor)	82.7 ( $\pm$ 2.6)	13 <sup>1</sup>	11
3 (Solid wall)	103.6 ( $\pm$ 3.6)	83.9	72
4 (Glazing)	174.2 ( $\pm$ 5.4)	13.3	11
5 (Roof)	180.5 ( $\pm$ 6.9)	7	6
6 (Baseline)	187.5 ( $\pm$ 7.6)	n/a	n/a

405  
406 The full retrofit resulted in a 63% reduction in the HTC of the Energy House from the baseline. The sum of the  
407 HTC reductions from the baseline for each thermal element retrofit measured in isolation (test stages 2, 3, 4,  
408 and 5) was 117.2W/K. This represents a discrepancy of 0.5% from the measured HTC reduction for the full  
409 retrofit from the baseline of 117.8 W/K. The close agreement between these values suggests that the  
410 boundary conditions were repeated throughout the experiment, resulting in precise HTC measurements. Such  
411 precision also allows the contribution of each thermal element to the HTC reduction to be disaggregated with  
412 confidence. In this experiment, the retrofit measure that achieved the greatest saving was the hybrid solid wall

<sup>1</sup> As the ground floor retrofit was not measured in isolation, its contribution to the HTC reduction was derived from the measured HTC change between test stage 1 and 2.

413 insulation applied to the external walls. This measure constituted 72% of the full retrofit HTC reduction.  
 414 Importantly, the results also show, that in this instance, undertaking a full retrofit all at once provides no  
 415 additional fabric heat loss improvement than would otherwise be achieved if the individual thermal elements  
 416 were retrofitted sequentially. It is unlikely such granularity could be achieved in the field to confidently report  
 417 these findings.

418 **3.2 In situ U-value measurements**

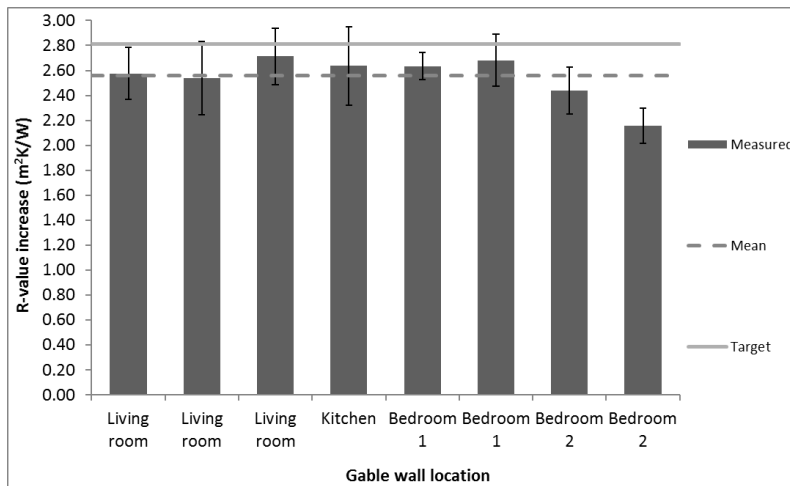
419 Table 6 provides a summary of the mean baseline and retrofit *in situ* U-values for each thermal element and  
 420 the target retrofit U-value calculated for each retrofit measure.

421 *Table 6 - Measured baseline and retrofit and target retrofit U-values for each thermal element*

Thermal element	U-value (W/m <sup>2</sup> K)		
	Baseline	Target retrofit	Measured retrofit
External wall (EWI)	1.74 (± 0.06)	0.30	0.33 (± 0.01)
External wall (IWI)	1.84 (± 0.08)	0.24	0.22 (± 0.01)
Roof (between joists)	0.35 (± 0.01)	0.15	0.16 (± 0.07)
Glazing (centre pane)	2.39 (± 0.09)	1.33	1.34 (± 0.05)
Ground floor (between joists)	0.61 (± 0.01)	0.12	0.13 (± 0.03)

422 From Table 6 it can be seen that the calculated target retrofit U-value was within the uncertainty bounds of  
 423 most thermal element's measured retrofit U-value, which suggests that retrofit measures performed close to  
 424 the calculated improvement at the locations measured. The exception were the external walls retrofitted with  
 425 EWI and IWI. The retrofitted front external wall retrofitted with IWI performed better than calculated.  
 426 However, this can be explained by the additional R-value resulting from the 10 mm unventilated airspace (0.15  
 427 m<sup>2</sup>K/W obtained from ISO 6946) created by the adhesive dabs used to affix the IWI to the inner surface of the  
 428 external walls which is not included in the BBA certificate. The baseline U-value of the gable external wall was  
 429 17% lower than the RdSAP default value of 2.10 W/m<sup>2</sup>K. In this instance retrofitting the external walls with  
 430 EWI reduced the U-value by 81%, calculating the U-value reduction on the default RdSAP baseline  
 431 performance and manufacturer's data predicts a saving of 86%. The discrepancy would be larger if EWI with a  
 432 lower R-value was applied and *vice versa*. This finding demonstrates the importance of measuring retrofit pre-  
 433 and post-retrofit to assess the change in fabric heat loss.  
 434

435 Comparing the difference in baseline and retrofit R-value enables a direct comparison with the R-value of the  
 436 applied retrofit materials at each location. Figure 4 shows the measured increase in the R-value from baseline  
 437 of the EWI retrofitted external wall at locations > 1 m from junctions and the calculated R-value improvement  
 438 for the EWI system. Two areas of notable underperformance on the gable external wall were identified from  
 439 the measurements (living room and bedroom 2), these became the focus of further investigation during the  
 440 blower door tests (refer to section 3.4).



441  
442 *Figure 4 – Measured increase in R-value of the gable external wall upgraded with EWI at locations > 1 m from*  
443 *junctions and the calculated R-value increase for the EWI system*

444 **3.3 Comparison of heat loss reductions using differing methods**

445 Table 7 compares differing methods for obtaining the total, fabric, and ventilation heat loss reductions  
446 resulting from the retrofit of individual thermal elements.

447 *Table 7 - Comparison of total, fabric, and ventilation heat loss reduction resulting from the retrofit of an*  
448 *individual thermal element using differing methods*

Thermal element retrofitted <sup>2</sup>	Reduction in heat loss from baseline (W/K)				
	Total		Fabric		Ventilation
	Aggregate method (coheating) (a)	Disaggregate method (b+c) <sup>3</sup>	Coheating & n <sub>50</sub> /19.2 derived (a-c)	U-value reduction*A (b) <sup>4</sup>	n <sub>50</sub> /19.2 derived (c)
Ground floor (test stage 2)	13	26.1	0	13.1	13
External walls (test stage 3)	83.9	93.1	81	90.2	2.9
Roof (test stage 5)	7	9.4	4.4	6.8	2.6

449 The reduction in total heat loss obtained using the disaggregate method is substantially greater than that  
450 obtained using the aggregate method (coheating HTC measurement) for each thermal element retrofitted. The  
451 discrepancy between the two values can be explained by questioning the values inputted into the disaggregate  
452 method calculation. The representative nature of the roof and ground floor U-values can be doubted as the  
453 heat loss observed across these elements showed greater variation than the external walls. The depth of the  
454 retrofitted mineral wool in the loft was inconsistent due to the shallow roof pitch and structural timber  
455 hindering the retrofit. In addition, Pelsmakers *et al* (2017<sup>38</sup>) also measured significant variation in the heat loss  
456 across the surface area of the Energy House ground floor. However, despite this, the greatest concern

<sup>2</sup> Replacement glazing excluded from this analysis as the effect of the window frame would have to be calculated for each window.

<sup>3</sup> Budgetary constraints prevented the calculation of the total heat loss from thermal bridging at junctions to include in the disaggregate method calculation.

<sup>4</sup> The U-value reduction for each thermal element was multiplied by its internal surface area. The U-value reduction for inhomogeneous thermal elements were area weighted to include the measured reduction in heat loss through the loft hatches and structural timber within the ceiling and ground floor.

457 surrounds the veracity of the  $n_{50}/19.2$  derived  $HTC_{(V)}$  approximation. The coheating and  $n_{50}/19.2$  derived fabric  
 458 heat loss approximation suggests that the ground floor retrofit provided no fabric thermal performance  
 459 improvement; this is in stark contradict to the *in situ* U-value measurements. The close agreement between  
 460 the fabric heat loss reduction derived from the *in situ* U-value measurements and the measured HTC reduction  
 461 for the roof and ground floor retrofits suggests that using 19.2 (or 20) as the divisor of  $n_{50}$  greatly  
 462 overestimates  $n$ , and a much higher divisor is required for the Energy House. It is thought that the lack of wind  
 463 within the environmental chamber during the tests resulted in a substantially lower background ventilation  
 464 rate than would normally be experienced by similar houses in the field. Therefore, it is likely that the measured  
 465 HTC of a home similar to the Energy House in the field would be greater due to a higher rate of wind driven  
 466  $HTC_{(V)}$ , lower  $R_{se}$ , and cooler void temperatures. The results also suggests that the ventilation heat loss rate  
 467 remained similar throughout the retrofit experiment, and that the reduction in HTC measured for each retrofit  
 468 measure would have been greater if the Energy House was exposed to wind, notably for the ground floor  
 469 where the retrofit delivered the greatest improvement in airtightness (refer to Table 8).

470 If one assumes that there was very little change in the  $HTC_{(V)}$  resulting from each retrofit measure, the  
 471 discrepancy between the external wall retrofit measured HTC reduction and the fabric heat loss reduction  
 472 derived from U-value measurements can be attributed to an increase in thermal bridging heat loss post-  
 473 retrofit, caused by the decision not to insulate the opening reveals. The fabric heat loss reduction derived from  
 474 *in situ* U-value measurements was based upon measurements taken > 1 m from junctions, so can be  
 475 considered reasonably unaffected by geometric thermal bridging. The normal distribution of baseline and  
 476 retrofit *in situ* U-values measured at these locations suggested a consistent rate of heat loss, confirming this  
 477 assumption. The distribution of *in situ* U-values which included measurements > 0.5 m from junctions was  
 478 normal for the baseline external wall, but displayed positive skew for the retrofit wall, suggesting an increase  
 479 in the influence of thermal bridging. This was confirmed by thermographic surveys and thermal bridging  
 480 calculations undertaken using Physibel TRISCO version 12.0w software (Physibel, 2010<sup>39</sup>), which predicted that  
 481 the window jamb  $\Psi$ -value increased post-retrofit from a baseline of 0.072 W/mK to 0.107 W/mK on the IWI  
 482 retrofitted front wall and IWI 0.206 W/mK on EWI retrofitted rear wall<sup>5</sup>. If the 6.3 W/K discrepancy is divided  
 483 by the external envelope area of 133.3 m<sup>2</sup>, it suggests an increase in  $\gamma$ -value of 0.05 W/m<sup>2</sup>K of the Energy  
 484 House following the external wall retrofit. It is doubtful whether the pre- and post-retrofit HTC and *in situ* U-  
 485 value measurements in the field would be accurate or precise enough to isolate such a change in  $\gamma$ -value.

### 486 3.4 Blower door tests

487 Table 8 provides  $q_{50}$  and  $n_{50}$  of the Energy House measured using a blower door test at each test stage of the  
 488 retrofit experiment and  $n$  estimated using  $n_{50}/19.2$ .

489 *Table 8 - Blower door test results showing reduction on baseline and  $n_{50}/19.2$  derived background ventilation*  
 490 *rate at each stage of the retrofit experiment*

Test stage	$q_{50}$ (m <sup>3</sup> .h <sup>-1</sup> .m <sup>2</sup> @ 50 Pa)	$q_{50}$ reduction on baseline (%)	$n_{50}$ (h <sup>-1</sup> @ 50 Pa)	$n$ (h <sup>-1</sup> )
1 (Full retrofit)	6.0 (± 0.1)	50	7.3 (± 0.1)	0.38
2 (Full retrofit with original floor)	10.4 (± 0.2)	42 <sup>6</sup>	12.5 (± 0.3)	0.65
3 (Solid wall)	11.1 (± 0.2)	8	13.4 (± 0.3)	0.70
4 (Glazing)	11.1 (± 0.2)	8	13.4 (± 0.3)	0.70
5 (Roof)	11.2 (± 0.2)	7	13.5 (± 0.3)	0.70

<sup>5</sup>Insulating the EWI reveals would have reduced the jamb  $\Psi$ -value to 0.045 W/mK.

<sup>6</sup> As the ground floor retrofit was not undertaken in isolation, the reduction from baseline was calculated as the measured  $q_{50}$  change between test stage 1 and 2.

6 (Baseline)	12.1 ( $\pm$ 0.2)	n/a	14.5 ( $\pm$ 0.3)	0.76
--------------	-------------------	-----	-------------------	------

491 The absence of wind within the chamber during the blower door tests meant that the measured air flow rate  
492 and induced pressure differential remained stable for each of the 12 tests (six for each pressurisation and  
493 depressurisation measurement) required to measure  $q_{50}$  and  $n_{50}$  at each stage of the retrofit experiment. This  
494 was signified by an  $r^2$  of 1 for each blower door test in which the same flow ring was in place for all  
495 measurements (test stages 1 and 6). The sheltered conditions increase confidence that the measurements  
496 were both accurate and repeatable and justifies the use of a 2% uncertainty value. The blower door tests  
497 measured a 50% reduction in  $q_{50}$  from baseline for the full retrofit. The ground floor retrofit resulted in the  
498 single greatest reduction in  $q_{50}$  of 42%. Air infiltration investigation during depressurisation using  
499 thermography suggested that the vapour membrane sealed to the walls, rather than the insulation between  
500 floor joists, was responsible for the scale of the reduction. This finding is consistent with those documented by  
501 Gillott *et al.* (2016<sup>40</sup>). A reduction in  $q_{50}$  from the baseline of the scale measured for the full and ground floor  
502 retrofits could be confidently detected in the field using blower door tests. However, the sensitivity of blower  
503 door test measurement accuracy to changes in wind velocity means that it is questionable whether the  
504 reductions in  $q_{50}$  of <10% achieved by retrofitting the other thermal elements could be measured with  
505 confidence in the field.

506 The blower door tests provided valuable insight for diagnosing the reasons for the measured  
507 underperformance of the EWI system. Thermocouples had been affixed to the outer leaf of the gable external  
508 wall prior to the installation of the EWI, in a 2 m horizontal array out from the junction with the IWI front wall,  
509 at intervals of 0.4 m and a height of 0.7 m above ground floor level. During blower door tests, the temperature  
510 measured at the interface between the outer leaf of brickwork and EWI 2 metres from the gable/front wall  
511 junction reduced. When a hairdryer was used to warm the air in the vicinity of the edge seal at the gable/front  
512 wall junction during depressurisation at 50 Pa, the interface temperature measured 2 m from the junction  
513 increased. This location corresponded to the area of greatest measured underperformance in the living room  
514 identified from the *in situ* U-value measurements.  $q$  measured in this region also took longer than better  
515 performing areas to return to a steady-state following a blower door test. From these observations, it was  
516 concluded that the EWI edge seal was not airtight, resulting in an air path between the chamber and the  
517 interface between the outer leaf of the external wall and EWI along the mortar joints to areas of poor contact  
518 between the EWI and uneven wall surface, enabling convective bypassing of the insulation layer. This finding  
519 provides evidence that poor edge sealing of mechanically fixed EWI boards without an adhesive coat reduces  
520 its performance. The observations made during the blower door tests suggest that thermal performance  
521 measurements in a test environment devoid of wind pressures could fail to identify the susceptibility of  
522 retrofit measures to a number of important heat loss mechanisms, such as wind washing, unless differing  
523 conditions are imposed upon the test subject. However, a steady-state environment prior to and following a  
524 blower door test enabled the use of temperature and  $q$  measurements to isolate where air movement within  
525 the building fabric had occurred during the test. Identifying air movement within the building fabric in the field  
526 from temperature and  $q$  measurements is inherently more complex and problematic due to the noise created  
527 by thermal mass effects.

#### 528 4. Conclusions

529 The Energy House test facility was found to enable the change in fabric heat loss resulting from the application  
530 of fabric retrofit measures to be measured to a level of accuracy which cannot be guaranteed in the field, due  
531 to the ability to precisely control external boundary conditions across successive test periods. Although the  
532 findings also suggest that the absence of wind within the environmental chamber underestimates the  
533 potential reduction in  $HTC_{(v)}$  resulting from improvements in airtightness, the test environment does enable  
534 the identification of other important heat loss phenomena, such as thermal bypassing, which may prove  
535 difficult to detect in the field. However, the absence of wind in the environmental chamber may mask the  
536 susceptibility of thermal elements to other thermal phenomena, particularly wind washing. Thus, the utility of  
537 the Energy House (and other full-scale test facilities) for testing the applicability of various thermal  
538 performance retrofit solutions to the field needs to be carefully considered. This is because the environmental  
539 chamber can never truly replicate the external environmental conditions experienced by houses the field, or

540 contain houses that are constructed in a manner truly representative of all the houses within its archetype.  
541 However, it is also the case that thermal performance test methods deployed in the field are not yet accurate  
542 or precise enough to fully account for the presence of a complex combination of dynamic and often interacting  
543 external boundary conditions. Additionally, no individual house in the field can ever be considered  
544 representative of an entire archetype. Therefore, the Energy House can be considered an incredibly useful  
545 facility for testing the effectiveness of a thermal fabric retrofit to a solid wall dwelling with characteristics  
546 similar to a sizable proportion of the UK's 'hard to treat' housing stock, providing those undertaking tests are  
547 aware of (or can adapt to) the limitations that come from testing within such an environmental chamber.

548 As the coheating test is based upon a steady-state energy balance, it was ideally suited for application in a  
549 steady-state test environment. As such, coheating tests can be undertaken over a much shorter duration than  
550 is possible in the field and they are not constrained by the heating season. *In situ* U-value measurements were  
551 also undertaken free from the uncertainty caused by thermal mass effects and the influence of direct solar  
552 radiation. Blower door tests at the Energy House test facility were not only more accurate than those generally  
553 undertaken in the field, but importantly, they also provided more potential for diagnosing the cause of  
554 underperformance by artificially inducing air movement. Since the experimental work detailed in this paper  
555 has been undertaken, fans have been installed within the environmental chamber that contains the Energy  
556 House to simulate wind upon the external façade of the Test House. It is suggested that future retrofit  
557 experiments undertake a number of steady-state measurements at a range of differing wind speeds, at each  
558 retrofit stage, to measure the change in thermal performance attributable to wind washing effects ( $R_{se}$  and the  
559 rate of ventilation in unconditioned voids would need to be measured).

560 During the tests, it was not possible to accurately compare HTC values for each test stage against a predicted  
561 HTC, as thermal bridging calculations were not performed for all junctions, and problems arose establishing n.  
562 Despite this, the change in HTC observed from coheating testing is considered the most robust measurement  
563 with which to assess the impact of retrofit, as it encapsulates the change in plane element U-value (especially  
564 non-homogeneous elements where obtaining representative measurements is difficult), thermal bridging at  
565 junctions,  $HTC_{(V)}$  and can account for other complex heat loss mechanisms, such as thermal bypassing and  
566 wind washing. Attempting to account for all of these heat loss mechanisms using disaggregated measurement  
567 techniques, is not practically possible or cost-effective. Further testing work at the Energy House should  
568 include calculation of all thermal bridges and a more robust method of determining the background ventilation  
569 measurement (e.g. a multi zone trace gas technique) should be used to enable the various heat loss  
570 mechanisms to be accurately disaggregated. Measuring the change in HTC resulting from heating of the  
571 underfloor void may also enable the suspended timber floor heat loss to be more accurately measured.

572 A recognised steady-state measurement standard for testing the thermal performance of a whole house or  
573 individual thermal element using a full-scale indoor test facility is needed. This would provide existing and  
574 future indoor full-scale facilities with the necessary requirements for boundary condition control and the  
575 method required to undertake steady-state measurements that can be considered acceptable for regulatory  
576 compliance.

## 577 **Acknowledgements**

578 We would like to thank Simon Gibson for project management of the retrofit. Special thanks go to Florent  
579 Alzetto and Callum Cuttle for lending their sizable brains to the project, and to Mo Benjaber for keeping the  
580 Energy House test facility running smoothly. Saint-Gobain for funding the retrofit experiment.

## 581 **References**

- 582 1. Marmot Review Team, (2011). *The Health Impacts of Cold Homes and Fuel Poverty*. Published by  
583 Friends of the Earth & the Marmot Review Team. London
- 584 2. DCLG (2017). English Housing Survey: Headline Report, 2015-16. Department for Communities and  
585 Local Government, UK Gov. Available from: [https://www.gov.uk/government/statistics/english-](https://www.gov.uk/government/statistics/english-housing-survey-2015-to-2016-headline-report)  
586 [housing-survey-2015-to-2016-headline-report](https://www.gov.uk/government/statistics/english-housing-survey-2015-to-2016-headline-report) [accessed: 10/03/2017]



- 587 3. Everett B. (2007). *Saving Energy: How to Cut Energy Wastage* in Elliot D et al. Sustainable Energy:  
588 Opportunities and Limitations. Energy, Climate and the Environment. Basingstoke, UK: Palgrave  
589 Macmillan. 108–134
- 590 4. Galvin, R. and Sunikka-Blank M. (2017) Ten questions concerning sustainable domestic thermal  
591 retrofit policy research. *Building and Environment*, 118, 377-388
- 592 5. Gupta, R., Gregg, M., Passmore, S. and Stevens, G. (2015) Intent and outcomes from the Retrofit for  
593 the Future programme: key lessons. *Building Research & Information*, 43,435-451.
- 594 6. Sunikka-Blank, M. & Galvin, R. (2012) Introducing the prebound effect: the gap between performance  
595 and actual energy consumption. *Building Research & Information*. 40 (3) 260-273
- 596 7. Galvin, R. (2014). "Making the 'rebound effect' more useful for performance evaluation of thermal  
597 retrofits of existing homes: Defining the 'energy savings deficit' and the 'energy performance gap'".  
598 *Energy and Buildings*; 69: 515–524.
- 599 8. Ofgem (2015) Energy Company Obligation 2015-17 (ECO2) Guidance: Delivery. December 2015.  
600 London, UK, Office of Gas and Electricity Markets.
- 601 9. Dowson, M., Poole, A., Harrison, D., & Susman, G. (2012). Domestic UK retrofit challenge: Barriers,  
602 incentives and current performance leading into the Green Deal. *Energy Policy*, 50, 294–305
- 603 10. BRE (2012), The Government's Standard Assessment Procedure for Energy Rating of Dwellings: 2012  
604 edition (updated Feb. 2014). Building Research Establishment, Watford: BRE on behalf of the  
605 Department for Energy and Climate Change.
- 606 11. BRE (2014) *In-situ measurements of wall U-values in English housing*. Report for the Department of  
607 Energy and Climate Change. Building Research Establishment, Watford. Available from <  
608 [https://www.gov.uk/government/uploads/system/uploads/attachment\\_data/file/409428/In-situ\\_u-](https://www.gov.uk/government/uploads/system/uploads/attachment_data/file/409428/In-situ_u-values_final_report.pdf)  
609 [values\\_final\\_report.pdf](https://www.gov.uk/government/uploads/system/uploads/attachment_data/file/409428/In-situ_u-values_final_report.pdf)> [Accessed 12/03/2017]
- 610 12. Francis G. N. Li, A.Z.P. Smith, Phillip Biddulph, Ian G. Hamilton, Robert Lowe, Anna Mavrogianni, Eleni  
611 Oikonomou, Rokia Raslan, Samuel Stamp, Andrew Stone, A.J. Summerfield, David Veitch, Virginia Gori  
612 & Tadj Oreszczyn (2015) Solid-wall U-values: heat flux measurements compared with standard  
613 assumptions, *Building Research & Information*, 43:2, 238-252, DOI: 10.1080/09613218.2014.967977
- 614 13. Doran, S. and Carr, B. (2008) *Thermal Transmittance of Walls of Dwellings Before and After*  
615 *Application of Cavity Wall Insulation*. A Report Prepared by BRE Scotland for the Energy Saving Trust,  
616 Report Number 222077, East Kilbride, UK, BRE Scotland.
- 617 14. Miles-Shenton D, Wingfield J, Sutton R & Bell M. (2011). Temple Avenue Project Part 2- Energy  
618 efficient renovation of an existing dwelling: Evaluation of design & construction and measurement of  
619 fabric performance. Report to Joseph Rowntree Foundation. Leeds Metropolitan University, Leeds.
- 620 15. BSI (2007) BS EN ISO 13789:2007 Thermal performance of buildings. Transmission and ventilation  
621 heat transfer coefficients. Calculation method. London. British Standards Institution
- 622 16. Jack, R., Loveday, D., Allinson, D. and Lomas, K. (2015) First evidence for the reliability of building  
623 coheating tests. *Building Research & Information* DOI:10.1080/09613218.2017.1299523
- 624 17. Rhee-Duverne, S. and Baker, P. (2013) Research into the thermal performance of traditional brick  
625 walls. English Heritage – Research Report. < [http://www.ewipro.co.uk/research-into-the-thermal-](http://www.ewipro.co.uk/research-into-the-thermal-performance-of-traditional-brick-walls.pdf)  
626 [performance-of-traditional-brick-walls.pdf](http://www.ewipro.co.uk/research-into-the-thermal-performance-of-traditional-brick-walls.pdf)>
- 627 18. BSI (2017) BS EN ISO 7345. Thermal performance of buildings and building components. Physical  
628 quantities and definitions. London. British Standards Institution
- 629 19. BSI (2014) BS ISO 9869-1 Thermal insulation. Building elements. In-situ measurement of thermal  
630 resistance and thermal transmittance. Heat flow meter method. London. British Standards Institution
- 631 20. Everett, R. (1985). Rapid Thermal Calibration of Houses, Technical Report, Open University Energy  
632 Research Group, Milton Keynes, UK, 1985, ERG 055.
- 633 21. Stamp, S., Lowe, R. and Altamirano, H. (2013) Using simulated co-heating tests to understand weather  
634 driven sources of uncertainty within the co-heating test method. In: (Proceedings) ECEEE. 3-8 June  
635 2013 (2049-2055).
- 636 22. Stamp, S., Altamirano-Medina, H. and Lowe, R. (2017) Measuring and accounting for solar gains in  
637 steady state whole building heat loss measurements. *Energy and Buildings*, 153, 168-178.
- 638 23. Persily, A. Repeatability and Accuracy of Pressurization Testing. In DOE/ASHRAE Conference 'Thermal  
639 Performance of the Exterior Envelopes of Buildings II', Las Vegas (1982).

- 640 24. ATTMA (2016) ATTMA Technical Standard L1. Measuring the Air Permeability of Building envelopes  
641 (Dwellings). September 2016. Northampton, UK, Air Tightness Testing and Measurement Association.
- 642 25. Bauwens, G. and Roels, S. (2014) Co-heating test: A state-of-the-art. *Energy and Buildings*, Volume 82,  
643 October 2014, p 163-172
- 644 26. Asdrubali, F. and Baldinelli, G., (2010) Thermal transmittance measurements with the hot box  
645 method: Calibration, experimental procedures, and uncertainty analyses of three different  
646 approaches. *Energy and Buildings*, 43, 1618-1626.
- 647 27. Wingfield, J., Johnston, D., Miles-Shenton, D. & Bell, M. (2010). *Whole house heat loss test method*  
648 *(Coheating)*. [Internet] Leeds, Leeds Metropolitan University. Available  
649 from [http://www.leedsbeckett.ac.uk/as/cebe/projects/coheating\\_test\\_protocol.pdf](http://www.leedsbeckett.ac.uk/as/cebe/projects/coheating_test_protocol.pdf) [Accessed  
650 10/03/2017]
- 651 28. Shipworth, M., Firth, S., Gentry, M., Wright, A., Shipworth, D. & Lomas, K. (2010) 'Central heating  
652 thermostat settings and timing: building demographics', *Building Research & Information*, 38, (1) 50-  
653 69
- 654 29. TSB (2010). The Technology Strategy Board Building Performance Evaluation, Domestic buildings –  
655 Guidance for project execution. Technology Strategy Board Swindon, UK
- 656 30. Johnston, D., Miles-Shenton, D., Farmer, D. & Wingfield, J. (2013) *Whole House Heat Loss Test Method*  
657 *(Coheating)*, Leeds Metropolitan University, 2013, June 2013. Available from:  
658 <http://www.leedsbeckett.ac.uk/as/cebe/#> [accessed 10/03/2017].
- 659 31. BSI (1994) BS ISO 9869 Thermal insulation. Building elements. In-situ measurement of thermal  
660 resistance and thermal transmittance. Heat flow meter method. London. British Standards Institution
- 661 32. BSI (2007) BS EN ISO 6946 Building Components and Building Elements – Thermal Resistance and  
662 Thermal Transmittance – Calculation Methods. Milton Keynes, British Standards Institution.
- 663 33. Kronvall (1978), Testing of houses for air leakage using a pressure method, *ASHRAE Transactions* 84  
664 (1) 72–79.
- 665 34. Sherman, M. H. (1987). Estimation of infiltration from leakage and climate indicators. *Energy and*  
666 *Buildings*, 10(1), 81–86.
- 667 35. Roulet, C., & Foradini, F. (2002). Simple and cheap air change rate measurement using CO2  
668 concentration decays. *International Journal of Ventilation*, 1(1), 39–44.
- 669 36. BSI (1987) BS ISO 9251 Thermal insulation. Heat transfer. Conditions and properties of materials.  
670 Vocabulary. London. British Standards Institution
- 671 37. BSI (1996) BS EN ISO 8990 Thermal insulation. Determination of steady-state thermal transmission  
672 properties. Calibrated and guarded hot box. London. British Standards Institution
- 673 38. Pelsmakers, S, Fitton, R, Biddulph, P, Swan, W, Croxford, B, Stamp, S, Calboli, F, Shipworth, D, Lowe, R,  
674 & Elwell, C (2017), 'Heat-flow variability of suspended timber ground floors: Implications for in-situ  
675 heat-flux measuring', *Energy and Buildings*, 138, pp. 396-405
- 676 39. Physibel (2010) Trisco Version 12.0w [Software] Maldegem: Physibel.
- 677 40. Gillott, M., Loveday, D., White, J., Wood, C., Chmutina, K., & Vadodaria, K. (2016), 'Improving the  
678 airtightness in an existing UK dwelling: The challenges, the measures and their effectiveness', *Building*  
679 *& Environment*, 95, pp. 227-239